Progress In Electromagnetics Research B, Vol. 21, 203–218, 2010

INTEGRAL METHOD FOR A CAPACITANCE MICROSCOPE THAT IS BASED ON CYLINDRIC METALLIC SURFACES

A. Mendoza-Suárez

Facultad de Físico-Matemáticas
Universidad Michoacana de San Nicolás de Hidalgo
Edificio "B", Ciudad Universitaria, C.P. 58060, Morelia, Michoacan, México

F. Villa-Villa

Centro de Investigaciones en Óptica A.C.
Lomas del Bosque 115, Col. Lomas del Campestre, C.P. 37150, León, Guanajuato, México

Abstract—In this work, we consider the problem of obtaining a capacitive image by scanning a "one-dimensional" surface of a closed conductor of arbitrary geometry. To solve our problem we propose a novel integral numerical method. The method is applied to different geometries by considering deterministic surfaces as complex as those with a fractal structure and random rough surfaces with Gaussian statistics. We find that the images obtained by simulating a prototype of a capacitive microscope, strongly depend on the interaction between the object and the probe. Despite this interaction, important information can be obtained regarding the statistical properties of the random roughness of the object surface.

1. INTRODUCTION

During the last two decades some research has been focused on considering the possibility of using capacitance as a variable to develop a scanning microscope that takes into account this physical quantity to measure capacitive images of different systems [1–7]. Until now some important results have been obtained by following a similar analysis applied to other microscopes like the scanning near field

Corresponding author: F. Villa-Villa (fvilla@cio.mx).

optical microscope (SNOM) [8] or the atomic force microscope [9], that are based on the scanning of a sharp tip in the vicinity of the surface under observation in the scale of a few tens of nanometers. In the case of capacitance microscopy, it is established a potential difference (a bias voltage) between the probe and the object. This constitutes a simple electrostatic capacitive system. Then, the capacitance can be measured for different relative positions between both conductors (the probe and the sample) and in this way a capacitive image is obtained.

At a small scale, the surfaces of physical objects present some roughness and some times it is convenient to model them by using the concept of random roughness with a given statistical properties. We are interested in considering a problem of capacitance microscopy that involves objects whose surfaces present a random roughness [10, 11]. In reference [10], Bruce et al. propose a system of open surfaces composed of two planes, one of them having some roughness. In reference [11] the authors consider the problem of analyzing the statistical parameters of random rough surfaces by using two different configurations: one with a plane probe and other with a plane having a Gaussian tip. It is worth to mention that to seek for an image and their statistical properties, they use an integral numerical method that involves periodic Green functions with open surfaces. This method is limited to non reentrant random rough surfaces (surface profiles defined by single-valued functions). The use of random surfaces is well known in the light scattering theory, where the models are limited to consider one-dimensional surfaces, that is the system has a cylindric symmetry along a given direction.

The idea of scanning a metallic tip across a surface of some nanometers to get a capacitive image of a sample has been applied successfully to measure the doping concentration in semiconductors [12–14]. On the other hand, during the last few years electrical capacitance tomography has been the subject of some study to get capacitive images of macroscopic volumetric objects with idea of monitoring and controlling industrial processes. In this case the object is put inside of a cylinder which has some electrodes on the curved wall that are set to a given electrostatic potential to determine for example the dielectric permittivity function on the surface of the object by measuring the capacitance of the system [15–18]. By taking the ideas from both capacitive systems, we will consider in this work a model to obtain capacitive images by scanning a closed conductor with a one-dimensional surface of arbitrary geometry. This problem involves the solution of Laplace's equation when boundary values for the electrostatic potential are specified. There exits different numerical methods to solve this equation and some of the most known employ

numerical relaxation [19]. This consists in a finite difference method that uses a point mesh to approximate numerically the derivatives appearing in Laplace's equation. The grid is used to span the space in a given domain. These methods would require huge computer resources in the case of random surfaces; besides, it could be a difficult problem to define a proper mesh of points in the case of deterministic surfaces with a complex geometry such as a fractal geometry.

To solve our problem we propose a novel integral numerical method that can be applied to those cases. This method is based on some ideas coming from the light scattering theory [20, 21] and some differential geometry concepts. The experience from the scattering theory shows that the integral methods are the most proper tools to consider random rough surfaces or surfaces with a fractal structure.

Concerning the possibility of extending our method to consider the three-dimensional case, we can say that it is quite possible if deterministic surfaces are involved [16]. However, as we are particularly interested in the problem of random surfaces; it is worth mentioning that in such case the problem becomes computationally prohibitive.

2. THEORY

Let us consider a metallic cylindric object with a transverse arbitrary section from which we can obtain a topography. If we now enclose the "sample" with a metallic concentric cylindric object that serves as a "probe" but being an extended object, this shell constitutes our probe.

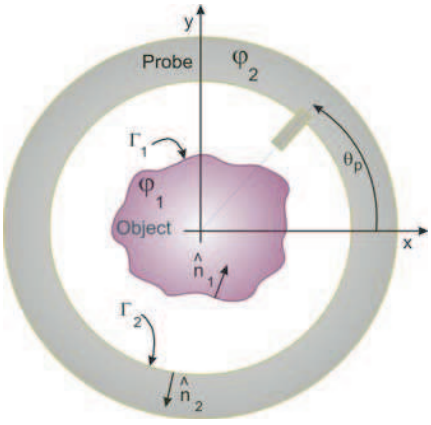

Figure 1. Schematic representation of the system probe-object.

In Fig. 1, we show a scheme of the transverse section of our probe with an object of irregular geometry. It is worth noticing that the transverse section of the probe is basically circular in this case, except for the small rectangular defect lying on it. This "rectangular tip" is positioned at different angular positions (θ_p) relative to the object to obtain an image. At each relative position of the probe and the object, we have a capacitance per unit length as a function of θ_p that can be numerically determined.

It is important to mention that when measuring, at each configuration the system must be kept static giving it enough time to get the electrostatic conditions.

To determine the capacitance as a function of the rotation angle we must solve basically the Laplace's equation,

$$\nabla^2\varphi = 0, \tag{1}$$

where ϕ is the electrostatic potential in the vacuum region between both conductors. In this work we consider Gaussian units.

The electrostatic potential φ must satisfy certain boundary conditions. We assume that φ has the values φ_1 and φ_2 on the surfaces of the sample and probe respectively (see Fig. 1). To solve the problem is convenient to use a Green function which is defined as the solution to the equation,

$$\nabla^2 G\left(\vec{r},\vec{r}\,'\right) = -4\pi\delta\,\left(\vec{r}-\vec{r}\,'\right). \tag{2}$$

It is well known that a possible Green function is given as the logarithmic function [10, 11]

$$G\,\left(\vec{r},\vec{r}\,'\right) = -2\ln\,\left(\left|\vec{r}-\vec{r}\,'\right|\right). \tag{3}$$

The functions φ and G satisfy the integral Green's theorem for two-dimensional systems

$$\iint\limits_{S}\left(\varphi\,\nabla^2 G - G\,\nabla^2\varphi\right)\,da = \oint\limits_{\Gamma_1+\Gamma_2}\left(\varphi\,\frac{\partial G}{\partial n} - G\frac{\partial\varphi}{\partial n}\right)ds, \tag{4}$$

where s is the arc length, S is the surface limited by the closed profiles Γ_1, Γ_2 (see Fig. 1) and $\hat{n}$ is the outward normal.

By applying the Gauss theorem we can obtain the charge density

$$\sigma_1 = \left.\frac{1}{4\pi}\frac{\partial\varphi}{\partial n_1}\right|_{\Gamma_1} \tag{5}$$

An analogous expression can be obtained for the charge density on the probe surface σ_2.

From Eqs. (4)–(5) and the boundary conditions, we obtain,

$$0 = \oint_{\Gamma_1} G\,\sigma_1\,ds + \oint_{\Gamma_2} G\,\sigma_2\,ds - \frac{\varphi_1}{4\pi}\oint_{\Gamma_1}\frac{\partial G}{\partial n_1}ds - \frac{\varphi_2}{4\pi}\oint_{\Gamma_2}\frac{\partial G}{\partial n_2}ds, \quad (6)$$

where σ_1 and σ_2 represent the charge densities on the surfaces with contours Γ_1 and Γ_2, respectively; while the normal derivatives of the Green functions are calculated by taking into account the normal to each surface $\hat{n}_1$ and $\hat{n}_2$, according to Fig. 1.

From the last expression we can formulate a numerical method following the outline given in reference [17]. By using this method we determine the charge density on each surface present in our system. With these results it is possible to calculate the capacitance on a given configuration.

To calculate the charge density we use a numerical method that is analogous to those integral methods formulated for light scattering by rough surfaces [20, 21]. The only difference here is that the Green functions are distinct. In this way, the Eq. (6) can be transformed to the following algebraic equations

$$b_i = \sum_{j=1}^{N_1} L_{ij}\sigma_{j(1)} + \sum_{j=1+N_1}^{N_1+N_2} L_{ij}\sigma_{j(2)}, \quad (7)$$

where $\sigma_{j(1)}$, $\sigma_{j(2)}$ denote the charge densities along the profiles Γ_1 and Γ_2, respectively (in the discrete case) and the inhomogeneous term b_i, is given by

$$b_i = \varphi_1 \sum_{j=1}^{N_1} M_{ij} + \varphi_2 \sum_{j=N_1+1}^{N_1+N_2} M_{ij}. \quad (8)$$

In the last two equations the matrix elements L_{ij} and M_{ij} are given by

$$L_{ij} = -2\,\Delta s \ln\left((X_i - X_j)^2 + (Y_i - Y_j)^2\right)(1-\delta_{ij}) - 2\,\Delta s \ln\left(\frac{\Delta s}{2e}\right)\delta_{ij}, \quad (9)$$

and

$$M_{ij} = \frac{\Delta s}{2\pi}\frac{\left(-Y_j'\,(X_i - X_j) + X_j'\,(Y_i - Y_j)\right)}{(X_i - X_j)^2 + (Y_i - Y_j)^2}(1-\delta_{ij}) + \left(\frac{1}{2} + \frac{\Delta s}{4\pi}\left(X_j'\,Y_j'' - X_j''\,Y_j'\right)\right)\delta_{ij}, \quad (10)$$

where Δs is the arc length between two consecutive points of a sampling (X_j, Y_j), along the profiles of the conductors; X_j' stands for the first derivative of the parametric function $X(s)$, evaluated at the

j-th point and X_j'' represents the second derivative; finally, δ_{ij} is the Kroenecker delta.

Once the charge density is obtained for a given configuration, it is possible to determine the positive charge per unit length induced on the surface of one of the conductors by direct numerical integration of the charge density. Finally, the capacitance per unit length is obtained by the ratio between this charge and the potential difference (assumed to be positive). Then, the capacitive image of the surface sample is given as a function of the angular position of the probe $C(\theta_p)$.

An object with a random rough surface can be represented by an ensemble of deterministic closed profiles (realizations). The statistics of the realization has the same properties of that corresponding to the random surface. The numerical generation of the closed realizations can be done using a method described elsewhere [21]. If a function $r(\theta)$, where $0 \leq \theta < 2\pi$, represents a given profile, let us consider the following properties: The average profile is a circumference of radius R, mathematically $\langle r(\theta) \rangle = R$.

We define a function

$$\rho(\theta) = r(\theta) - R, \tag{11}$$

where $\rho\,(\theta)$, represents the variation of a radial profile with reference to a circumference of radius R. The random surface can be modeled by considering a Gaussian distribution given by

$$f\,(\rho) = \frac{1}{\sqrt{2\pi\zeta}} \exp\left(-\frac{\rho^2}{2\zeta^2}\right), \tag{12}$$

where ζ represents the standard deviation of the distribution $f(\rho)$.

By defining the angular correlation function as

$$B(\theta,\, \theta') = \frac{1}{\zeta^2} \left\langle \rho(\theta)\, \rho(\theta') \right\rangle. \tag{13}$$

We assume that this correlation function has a Gaussian form

$$B\left(\theta, \theta'\right) = \exp\left(-\frac{(\theta - \theta')^2}{\Theta^2}\right), \tag{14}$$

where Θ stands for the "angular correlation length" and represents the angular scale of the random roughness.

An ensemble of profiles with the required statistical properties can be numerically generated from the following expression

$$\rho(\theta_k) = \zeta \sum_{j=-\infty}^{+\infty} \left(\frac{2\Delta\theta}{\Theta\sqrt{\pi}}\right)^{1/2} \exp\left(\frac{-2\,(\Delta\theta)^2 j^2}{\Theta^2}\right) X_{j+k}. \tag{15}$$

Here X_j represents Gaussian variables with zero media and standard deviation equal to one, θ_k is a discrete value of θ given as $\theta_k = k\,\Delta\theta$ being $k = 0, 1, 2, \ldots n$, where n stands for the number of sampling points and $\Delta\theta$ is angular step.

3. NUMERICAL RESULTS

To test our formalism, let us consider the case when the profiles of the sample and the probe are circumferences of radius $r_1 = 1$ and $r_2 = 2$ (arbitrary units), respectively; while the potentials of the conductor surfaces are $\varphi_1 = 0$ and $\varphi_2 = 1$. This case corresponds to the calculation of capacitance per unit length of a capacitor of cylindric surfaces of infinite length. The analytical result in this case is given as $0.5(\varphi_2 - \varphi_1)/\ln(r_2/r_1) = 0.721$, which is very close to that obtained numerically, 0.7264, by using the proposed formalism. Additionally, in Fig. 2, we show the electrostatic potential in a given radial direction in the vacuum region between both conductors. The dashed curve corresponds to the analytical result $\varphi = (\varphi_2 - \varphi_1)\ln(r/r_1)\ln(r_2/r_1) + \varphi_1$ and the solid curve is associated to the numerical calculations. It is important to notice that the agreement is so good that only one curve can be appreciated.

In Fig. 3, we show the profile Γ_2 of the conductor that plays the

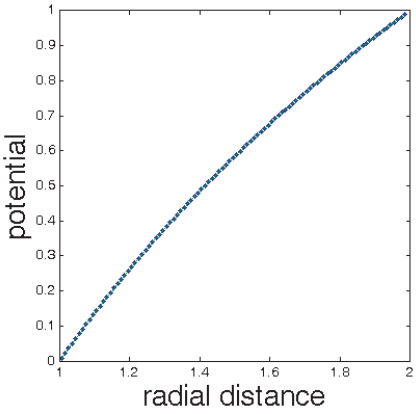

Figure 2. Comparison between the analytical (dashed curve) and numerical (solid curve) results for the electrostatic potential as a function of radial distance.

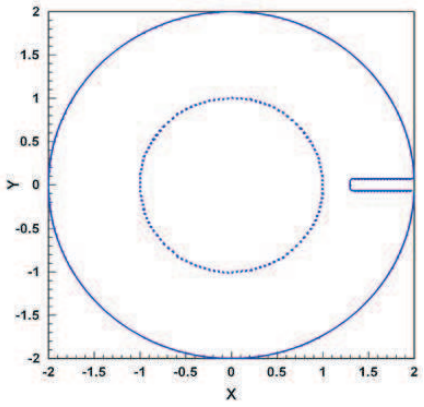

Figure 3. Profiles of the probe (external contour) and the object (internal profile).

role of the probe (external profile). The profile is circular except for a rectangular "tip" of length 0.7 and 0.14 wide that is used to inspect the object. In this case, the object Γ_1 is perfectly circular (internal profile).

At this point is important to mention that in the case of the typical capacitance microscopy the tip used has a triangular or pyramidal shape. As we are considering a tip that could be used even with a macroscopic system the probe can be rectangular. We compared the results obtained by using both tips obtaining better resolution with the rectangular shape. In any way, with our method we are able to model probes with any geometry.

The radius of the probe and the object are the same as those used in the previous example. The image of the object surface is given by $C(\theta_p)$. In polar coordinates this function results to be as expected, a circumference (see Fig. 4). So, we want to point out that the presence of the probe is necessary to get a capacitance image. The value of the capacitance in this case is 0.7069. Let us compare this result with that of the previous example 0.7264. As it becomes evident, the capacitance change is due to a change produced on the probe. This shows that the image of a given object is dependent on the geometry of the probe and such fact complicates the interpretation of obtained images.

As another application example, let us consider the case of an object with circular transverse section having a rectangular defect of length 0.2 and 0.21 wide. In Fig. 5, we show the contours of our object and the probe. We keep the same parameters of previous examples.

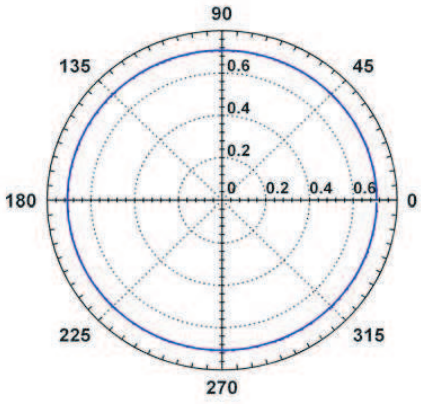

Figure 4. Object image corresponding to the geometry of Fig. 3 (solid curve).

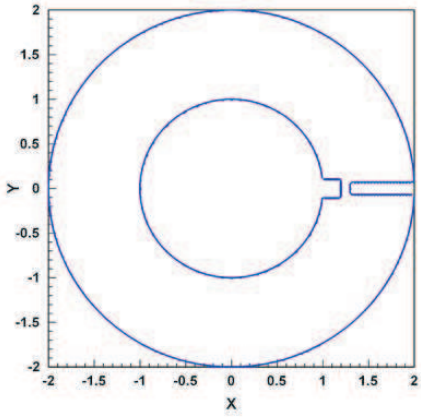

Figure 5. Transverse sections of the probe and the object with a small defect.

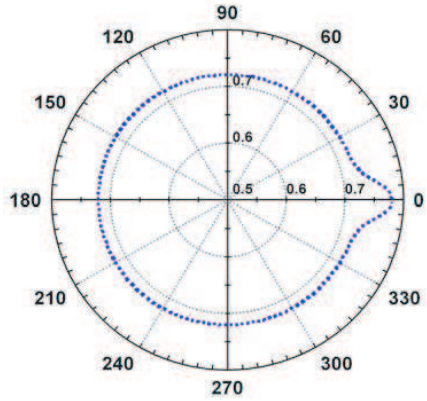

Figure 6. Object image of the set up shown in Fig. 5.

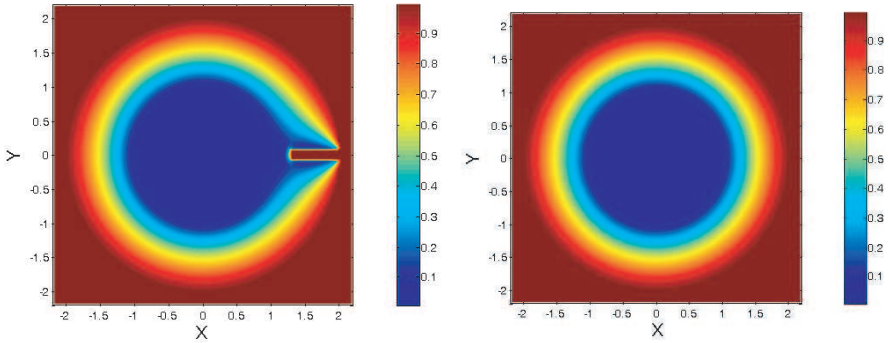

Figure 7. (a) Electrostatic potential for the system given in Fig. 5. (b) Electrostatic potential in the case of a cylindric capacitor.

In Fig. 6, we show the image corresponding to this case. It is worth noticing that from the image it is easy to deduce that the object has a localized symmetric protuberance. However, from this image, the exact shape of this defect can not be obtained by a simple operation.

The electrostatic potential corresponding to the system given in Fig. 5 is shown in Fig. 7(a). We have included the case of the cylindric capacitor in Fig. 7(b) in order to visually compare the differences between both cases.

It is worth to observe that the electrostatic potential has appreciable changes in the vicinity of the probe and object defect only.

We can infer from Fig. 7 that the electric field is quite intense near the probe surface. The electrostatic potential around the probe and beyond this near zone becomes perturbed and lowered (comparatively speaking) in this region.

Since, the resolution is dependent on the distance between the

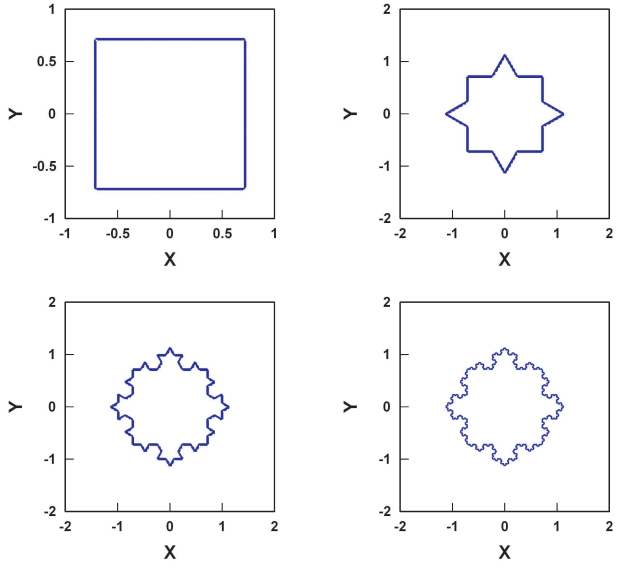

Figure 8. Objects with Koch triadic prefractal profiles.

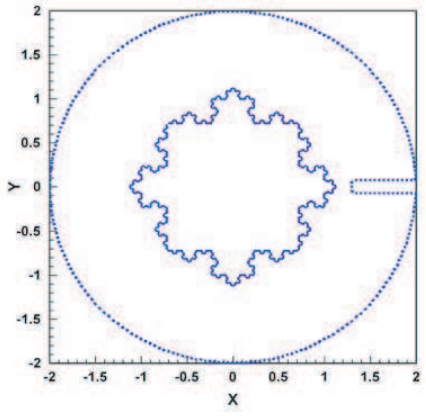

Figure 9. Capacitance microscope showing an object whose transversal section has a fractal structure.

probe and the object, those structure details that are closer to the probe are better resolved in the image than those that are located farther, this effect is known as the shadowing effect in the literature [11]. Even though the fine structure details are close to the probe, they can not be perfectly solved. This becomes evident from the image in the region of the protuberance, where the edges have been smoothed and the rectangular shape of the defect has been widened. These results will be useful to understand the image of complex objects as we will see below.

Let us now consider objects with more complex geometric structure like those having transversal sections with Koch triadic prefractal profiles [20] of order 0, 1, 2, 3 and 4 respectively (see Fig. 8 for the four first orders). In these cases the microscope is shown in Fig. 9.

The effects on the capacitance image of an object with prefractal geometry are shown in Fig. 10 for different prefractal orders. As mentioned in the previous paragraph, it is evident that fine structure can not be resolved clearly.

The corners of the square (order 0, solid curve in Fig. 10) can be appreciated in the capacitance image and even the vertices

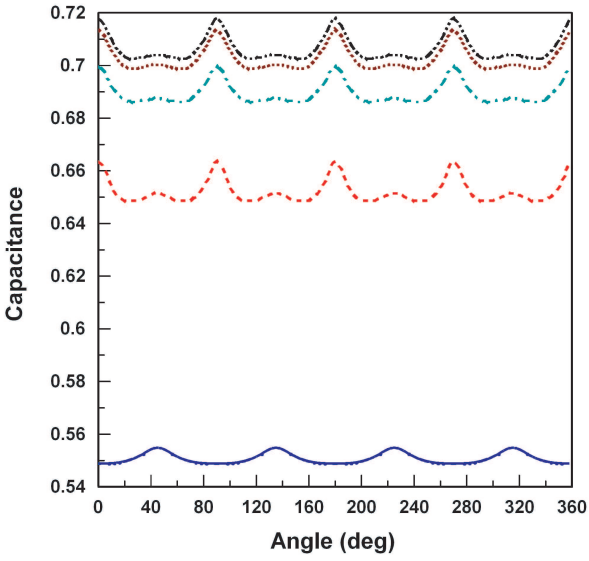

Figure 10. Capacitance image for objects with fractal orders 0 (solid curve), 1 (dashed curve), 2 (dot-dashed curve), 3 (dotted curve), 4 (dot-dot-dashed curve).

corresponding to the object of order 1 (dashed curve). Beyond order 1 the prefractal fine structure can not be appreciated, however, it is important to notice that the curves are displaced to upper capacitance values as we go to upper fractal orders. So, the microscope is able to distinguish a difference between the object with fractal structures of order 4 and 5 (dotted and dot-dot-dashed curves respectively).

Since the capacitance depends on the geometric structures as a whole, the method is sensitive to the presence of fine structure around the object. So, the instrument could be capable of detecting contamination on the surface of a real object, for instance.

As a last example let us consider an object having a random rough surface with a Gaussian statistics. In Fig. 11, it is shown the object (internal profile) that represents one realization of an ensemble associated to the object surface. We took in this work an ensemble of 1000 realizations that was appropriate to obtain stable results. The surface statistics is characterized by two parameters: the height standard deviation and the angular correlation length. These parameters have the values 1/30 and 10°, respectively. Despite this standard deviation seem to be small, the profile of a given realization can deviate considerably from the average circumference in some directions.

In Fig. 12, we show the corresponding image obtained by this microscope. The image has some similarities to the object itself. It is worth to observe that some fine details of the structure are lost due to the effects mentioned in the previous example.

Considering the Gaussian statistics of the random surface we can

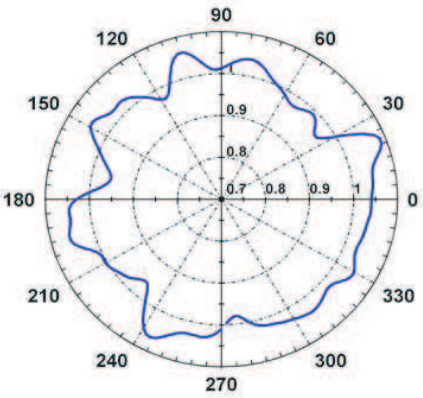

Figure 11. One realization of object surface.

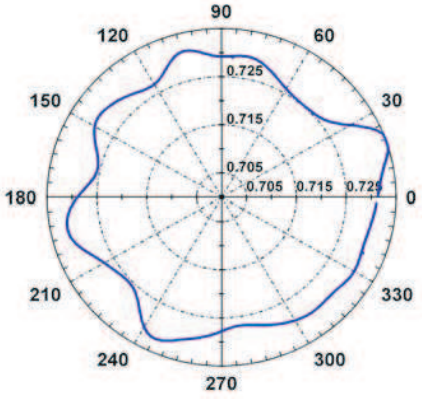

Figure 12. Image of the object surface given in Fig. 9.

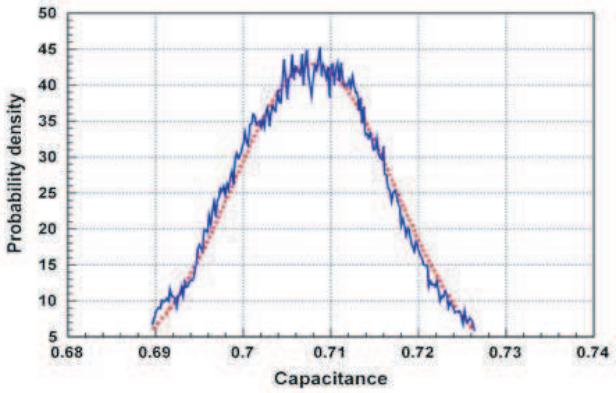

Figure 13. Comparison of the Gaussian probability density (dashed curve) with that determined numerically (solid curve).

ask about the possibility of extracting some information regarding the statistical properties of the ensemble of images. We can just conjecture that the statistics of this ensemble should be Gaussian. To conclude something about this conjecture, let us consider Fig. 13, where we show two curves, the first one corresponds to the probability density (solid curve) associated to a radial direction of the images when represented in polar coordinates. This probability density is averaged over 180 discrete values that we considered for $\theta_p = 0°,\ 2°, \ldots 358°$. With the data of this curve we obtained an average of 0.708 and a standard deviation of 0.009. The second graphics (dashed curve) constitutes a Gaussian distribution with these parameters. We can notice the good agreement of both curves.

In a similar fashion in Fig. 14, we show the comparison between the correlation function (averaged over θ') numerically determined (solid curve) from the ensemble of images and the function (dashed curve)

$$B_C(\theta) = a + b \exp\left(-\frac{\theta^2}{\Theta_c^2}\right), \tag{16}$$

where $a = 0.928$, $b = 0.072$ and $\Theta_c = 17.454°$. This is not by far a Gaussian function, however, a translation and rescaling of this function, gives us a function similar to that given in Eq. (14) with $\theta' = 0$.

We can conclude from our comparison that in this case we don not have a perfect Gaussian statistics. However, attributing these rescale and translation parameters in part to the configuration of the microscope itself, in principle it is possible to deduce the Gaussian character of the random surface.

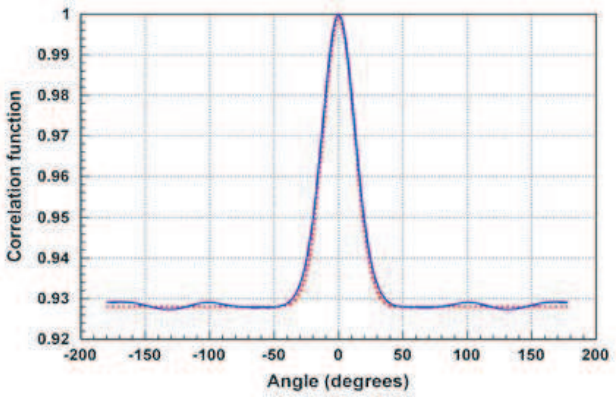

Figure 14. Comparison of the correlation function with that determined numerically (solid curve).

4. CONCLUSION

We conclude that with our model, we are able to obtain images from objects with closed surfaces that can be deterministic or random as well. The images were obtained by graphing the capacitance of a system of two concentric conductors of cylindric shape (probe and object) at different angular positions of the probe. We found that, in the case of simple objects the resolution of the images strongly depend on the shadowing effect.

If the object is of complex topography like that of a random rough surface, the image is also complex but preserves the general details depending on the shadowing. Even though the statistics of the surface object is Gaussian we found that the statistics of the capacitance images is not perfectly Gaussian. Particularly referring to the angular correlation function of the images ensemble, it has an essentially Gaussian shape but displaced and rescaled.

To obtain the relation between the height standard deviation and the angular correlation length of the ensemble of images and those corresponding to the ensemble of object realizations is a complex task that deserves a future work.

ACKNOWLEDGMENT

We appreciate the partial support given by the CIC-UMSNH through the Grant 9.2 received for the realization of this work.

REFERENCES

1. Bugg, C. D. and P. J. King, "Scanning capacitance microscopy," *J. Phys. E: Sci. Instrum.*, Vol. 21, 147–151, 1988.
2. Williams, C. C., W. P. Hough, and S. A. Rishton, "Scanning capacitance microscopy on a 25 nm scale," *Appl. Phys. Lett.*, Vol. 55, 203–205, 1989.
3. Gómez-Moñivas, S., J. J. Sáenza, R. Carminati, and J. J. Greffet, "Theory of electrostatic probe microscopy: A simple perturbative approach," *Appl. Phys. Lett.*, Vol. 76, 2955–2957, 2000.
4. Jaensch, S., H. Scmidt, and M. Grundmann, "Quantitative scanning capacitance microscopy," *Physica B*, Vol. 376–377, 913–915, 2006.
5. García-Valenzuela, A., N. C. Bruce, and D. Kouznetsov, "An investigation into the applicability of perturbation techniques to solve integral equations for a parallel-plate capacitor with a rough electrode," *J. Phys. D: Appl. Phys.*, Vol. 31, 240–251, 1998.
6. Bruce, N. C., A. García-Valenzuela, and D. Kouznetsov, "Perturbation theory for surface-profile imaging with a capacitive probe," *Appl. Phys. Lett.*, Vol. 77, 2066–2068, 2000.
7. Bruce, N. C., A. García-Valenzuela, and D. Kouznetsov, "The lateral resolution for imaging periodic conducting surfaces in capacitive microscopy," *J. Phys. D: Appl. Phys.*, Vol. 33, 2890–2898, 2000.
8. Setala, T., M. Kaivola, and A. T. Friberg, "Evanescent and propagation electromagnetic fields in scattering from point-dipole structures," *J. Opt. Soc. Am. A*, Vol. 18, 678–688, 2001.
9. Beladi, S., P. Girard, and G. Leveque, "Electrostatic forces acting on the tip in atomic force microscopy: Modelization and comparison with analytic expressions," *J. Appl. Phys.*, Vol. 81, 1023–1030, 1997.
10. Bruce, N. C., A. García-Valenzuela, and D. Kouznetsov, "Rough-surface capacitor: Approximations of the capacitance with elementary functions," *J. Phys. D: Appl. Phys.*, Vol. 32, 2692–2702, 1999.
11. Bruce, N. C. and A. García-Valenzuela, "Capacitance measurement of Gaussian random rough surfaces with planar and corrugated electrodes," *Meas. Sci. Technol.*, Vol. 16, 669–676, 2005.
12. Marchiando, J. F. and J. J. Kopanski, "Regression procedure for determining the dopant profile in semiconductors from scanning capacitance microscopy data," *J. Appl. Phys.*, Vol. 92, 5798, 2002.

13. Giannazzo, F., D. Goghero, V. Raineri, S. Mirabella, and F. Priolo, "Scanning capacitance microscopy on ultranarrow doping profiles in Si," *Appl. Phys. Lett.*, Vol. 83, 2659, 2003.
14. Giannazzo, F., D. Goghero, and V. Raineri, "Experimental aspects and modeling for quantitative measurements in scanning capacitance microscopy," *J. Vac. Sci. Technol. B*, Vol. 22, 2391, 2004.
15. Banasiak, R., R. Wajman, D. Sankowski, and M. Soleimani, "Three-dimensional nonlinear inversion of electrical capacitance tomography data using a complete sensor model," *Progress In Electromagnetic Research*, PIER 100, 219–234, 2010.
16. Wang, C.-F., L.-W. Li, P.-S. Kooi, and M.-S. Leong, "Efficient capacitance computation for three-dimensional structures based on adaptive integral method," *Progress In Electromagnetic Research*, PIER 30, 33–46, 2001.
17. Goharian, M., M. Soleimani, and G. Moran, "A trust region subproblem for 3D electrical impedance tomography inverse problem using experimental data," *Progress In Electromagnetic Research*, PIER 94, 19–32, 2009.
18. Soleimani, M., C. N. Mitchell, R. Banasiak, R. Wajman, and A. Adler, "Four-dimensional electrical capacitance tomography imaging using experimental data," *Progress In Electromagnetic Research*, PIER 90, 171–182, 2009.
19. Press, W. H., S. A. Teukolsky, W. T. Vetterling, and B. P. Flannery, *Numerical Recipes in Fortran 77*, 2nd edition, Cambridge University Press, New York 2003.
20. Mendoza-Suárez, A. and E. R. Mendez, "Light scattering by a reentrant fractal surface," *Appl. Opt.*, Vol. 36, 3521–3531, 1997.
21. Mendoza-Suárez, A., U. Ruíz-Corona, and R. Espinosa-Luna, "Effects of wall random roughness on TE and TM modes in a hollow conducting waveguide," *Opt. Comm.*, Vol. 238, 291–299, 2004.